

# Enhancing LV System Resilience through Probabilistic Forecasting of Interdependent Variables: Voltage, Reactive and Active Power

Anthony FAUSTINE  
Center for Intelligent Power (CIP)  
Eaton corporation, Dublin, Ireland  
sambaiga@gmail.com

Lucas PEREIRA  
ITI, LARSyS  
Técnico Lisboa, Portugal  
lucas.pereira@tecnico.ulisboa.pt

## Abstract

This paper presents a probabilistic forecasting approach tailored for low voltage (LV) substations, offering short-term predictions for three crucial variables: voltage, reactive power, and active power. These parameters play a vital role in the resilience of distribution systems, especially in the presence of Distributed Energy Resources (DERs). Evaluation with simulated data shows that active and reactive power forecasts degrade notably with higher EV penetration, whereas voltage forecasting experiences less degradation across all scenarios.

## 1. INTRODUCTION

The power grid is undergoing a significant transformation driven by the critical goal of mitigating climate change. This energy transition has led to a surge in the diversity and integration of Distributed Energy Resources (DERs), such as Renewable Energy Source (RES), Electric Vehicle (EV)s, and Battery Energy Storage System (BESS), into the Low Voltage (LV) distribution network. While DERs integration presents exciting opportunities to enhance LV resilience, it also introduces significant challenges. LV resilience refers to the network's ability to withstand and recover from disruptions while maintaining reliable and high-quality power delivery [1].

Specifically, the proliferation of Photovoltaic (PV) systems, can lead to periods of excess generation, creating a "duck curve" in the net-load profile [2]. This overgeneration can cause power quality fluctuations, voltage swings, or grid stress. Concurrently, increasing peak demand from the growing number of EVs and Electric Heating Systems (EHS) leads to congestion, especially during peak hours [3], [4]. This results in increased power losses, phase imbalances, overloading, and voltage drops, potentially causing outages.

Despite these challenges, well-managed DERs can improve LV resilience. For instance, RES with BESS [5], [6] or Vehicle to Grid (V2G) technology [7] can provide backup power during outages [8] or help control

peak demands [5] or voltage fluctuation [9]. Additionally, with more DERs, the grid becomes less reliant on a single point of failure, such as a large power plant outage.

Effective management of DERs for resilience improvement depends on the ability to predict future demand and generation and use this prediction to make informed decisions and control strategies. As such, forecasting demand and generation is the key to enhancing resilience in LV power grids amid the energy transition. More precisely, to ensure the resilience of LV distribution systems, Distribution System Operator (DSO)s need comprehensive insights into voltage, reactive power, and active power [10], [11]. Voltage forecasts help anticipate and mitigate potential issues through proactive regulation strategies [10], while reactive and active power forecasts identify peak demand periods, load imbalances, and potential overloads [11].

Most existing forecasting methods in power systems rely on univariate point forecasts, which predict a single value without estimating inherent uncertainty. This lack of uncertainty quantification can lead to suboptimal decision-making and increased risks in LV system operations [12]. Additionally, these methods require separate models for each target variable (voltage, reactive power, and active power), which, besides being inefficient and resource-intensive, fail to capture the interdependencies between variables [13].

To address these challenges, this paper presents a novel framework for producing multivariate probabilistic forecasts of three critical, interdependent variables at LV substations: voltage, reactive power, and active power. Our approach leverages a lightweight neural network architecture inspired by [12] to capture the quantile distribution of these variables. This enables highly accurate, very short-term, and short-to-medium-term forecasts that account for prediction uncertainty.

The proposed framework is evaluated through a series of simulated low-voltage (LV) secondary substation scenarios, each featuring varying combinations of photovoltaic (PV) and electric vehicle (EV) penetration levels. This approach facilitates a comprehensive assessment of the impacts of PV and EV integration on forecasting performance.

## 2. METHODS

We leverage neural network-parameterised Quantile regression (QR) regression to generate probabilistic forecasts. QR is an effective non-parametric method for estimating uncertainty in load forecasting, capable of modeling complex distributions without assuming an underlying data distribution [12], [14].

$$p(\mathbf{y}_H | \mathbf{x}_L, \mathbf{c}_T) = \{Q_\theta(\tau_{im}^1), Q_\theta(\tau_{im}^2) \dots Q_\theta(\tau_{im}^N)\} \quad (1)$$

where  $\tau \in [0, 1]$  is a set of  $N \times H \times M$  quantile probabilities satisfying:

$$\tau_{im}^1 < \tau_{im}^2 < \dots < \tau_{im}^{N-1} < \tau_{im}^N \quad (2)$$

$t = \{1 \dots H\}$  and  $m = \{1 \dots M\}$  equal to the number of variables being predicted which is 3 in this case.  $Q_\theta(\tau)$  is  $N \times H \times M$  quantile functions characterised by  $p(\mathbf{x} \leq Q_\theta(\tau))$ . Thus QR quantifies predictive uncertainty by providing a prediction interval  $[Q_\theta(\tau_{im}^L), Q_\theta(\tau_{im}^U)]$ , which includes lower ( $L$ ) and upper ( $U$ ) quantile bounds within which predictions are expected to fall.

The proposed multivariate QR approach leverages a Scalable Multilayer Perceptron Forecasting (MLPF), building upon the work presented in [12], to learn quantile fractions and their associated values. This enables the generation of forecasts along with their predictive uncertainty as illustrated in Fig. 1. Users simply specify

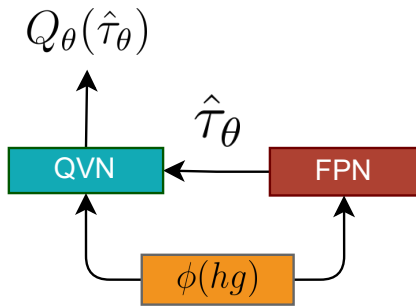


Figure 1: The full parameterised QR with two neural network blocks, namely Quantile Value Network (QVN) and Fraction Proposal Network (FPN), which jointly learn both the quantile values and quantile fractions.  $\phi(hf)$ , is the feature representation, obtained from MLPF encoders.

the desired number of quantiles, and the model automatically learns the optimal quantile probability  $\tau_{im}^*$  and corresponding values  $Q_\theta(\tau_{im}^*)$  that best characterize the forecasted variables.

## 3. EXPERIMENTAL DESIGN

### 3.1. Simulation of Scenarios

We implemented a simulation of a four-feeder LV system using the Hybrid European MV–LV Network Models [15]. Simulated data was generated for 365 days,

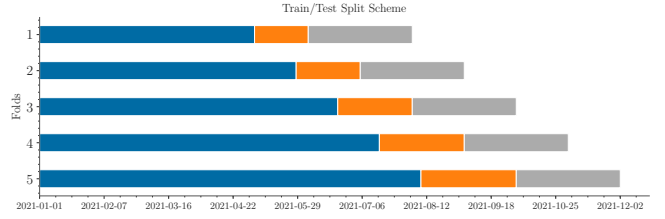


Figure 2: 5-folds cross backtesting cross validation

with a sample interval of 30 minutes. The OpenDSS simulator was employed in a time series model for the simulations.

Multiple simulation runs were conducted with varying DER adoption rates. Specifically, the adoption rates for photovoltaic (PV) and electric vehicle (EV) systems were independently varied across the following values: 0%, 20%, 40%, 60%, and 80%. For each end consumer in the LV network, we assumed a PV system with a 3 kVA inverter rated for a maximum output power of 3 kW. Real-trace data of normalized PV generation recorded from households in the AusNet grid<sup>1</sup> was used as input to the PV system. Similarly, a real EV charging power trace obtained from [16] was used to represent EV charging behavior and its impact on the LV networks. Additionally, real power trace data recorded from households in the AusNet grid was used to create the baseline power consumption profile of each connected end consumer.

### 3.2. Training and Testing Procedures

For training and testing the proposed forecasting methods, this work uses a 5-folds back-testing cross-validation with an expanding window as illustrated in Fig. 2. For this set-up we set the initial historical period to at least 6 months and the fixed future time window is set to 2 months [17]. The sliding window is extended by 1 month as we move forward in the time series. Each model is trained on 90% of the training window for 100 iterations and validated on the remaining 10%.

We assess the forecasting performance using Symmetric Mean Absolute Percentage Error (SMAPE) and Coverage Width and Forecasting Error based metric (CWE) metrics. SMAPE is the point forecast point metric expressed as a percentage defined as

$$\text{SMAPE} = \frac{1}{T} \sum_{t=1}^{t=T} \frac{2|\hat{y}_t - y_t|}{(|y_t| + |\hat{y}_t|)} \quad (3)$$

Unlike other percentage metrics like Mean Absolute Percentage Error (MAPE), SMAPE treats overestimation and underestimation equally by using the sum of actual and predicted values as the scaling factor, making it a more balanced measure than other metrics. SMAPE is bounded between 0 and 2, with 0 representing the best performance and 2 indicating the poorest performance.

<sup>1</sup><https://www.ausnetservices.com.au/>

On the other hand, the CWE metric introduced in [17] is a probabilistic metric that incorporates two essential elements of probabilistic forecast: Predictive Interval Coverage Probability (PICP) and Normalized Mean Prediction Interval width (NMPI). NMPI (Eq. (4)) measures the average width (sharpness) of the prediction interval, whereas PICP measures the proportion of times that the observed value falls within the predicted interval.

$$\text{NMPI} = \frac{1}{R} \text{median}(C_1^U - C_1^L, \dots, C_H^U - C_H^L) \quad (4)$$

$$\text{PICP} = \frac{1}{H} \sum_{t=1}^H \mathbb{I}(y_t \in [C_t^U, C_t^L]) \quad (5)$$

where  $C_t^L$  and  $C_t^U$  represent lower and upper predictive intervals and  $R = \max\{y_1, \dots, y_H\}$ . The CWE metric is defined as the harmonic mean between  $\gamma_{picp}$  a measures that quantify the misscoverage rate from the ideal coverage probability  $1 - \alpha$  and  $\gamma_{nmpi}$  a measures of deviation from the ideal predictive interval width (efficiency).

$$\text{CWE} = 2 \frac{\gamma_{nmpi} \cdot \gamma_{picp}}{\gamma_{picp} + \gamma_{nmpi}} \quad (6)$$

where:

$$\gamma_{picp} = \frac{\Delta_{picp} - \alpha}{1 - \alpha} \quad (7)$$

$$\Delta_{picp} = \begin{cases} (\text{PICP} + \alpha - 1) & \text{if } \text{PICP} \leq 1 - \alpha \\ 1 & \text{otherwise} \end{cases} \quad (8)$$

$$\gamma_{nmpi} = \frac{1 - \Delta_{nmpi}^2}{1 + \Delta_{nmpi}} \quad (9)$$

$$\Delta_{nmpi} = \left| \text{NMPI} - \frac{\kappa}{R} \right| \quad (10)$$

## 4. RESULTS

The forecasting results are presented in Figs. 3 to 5. The study reveals that for active power (Fig. 3), the impact on forecasting performance tends to stabilize after 20% PV penetration compared to the initial increase from zero to 20%. Concerning Q (Fig. 4), the impact of increasing PV on forecasting performance is much smaller, with values around 0.25 SMAPE, independently of the PV generation rates.

It can also be observed that both active and reactive power forecasts degrade more rapidly with increased EV penetration, particularly at 80% EV penetration, where the error approaches 0.75 SMAPE. Higher EV penetration also leads to a decrease in conditional weighted error (CWE), making predictive intervals less conclusive. Interestingly, beyond 20% penetration of PV and EV, CWE exhibits similar degradation despite the more pronounced decrease in forecasting performance.

Regarding voltage (Fig. 5), the forecasting quality is less affected by increased PV but deteriorates faster

with more EVs, although the variation in CWE remains moderate, indicating a balanced predictive interval. Notably, even with zero PV, having over 20% EVs can significantly impair voltage forecasting performance.

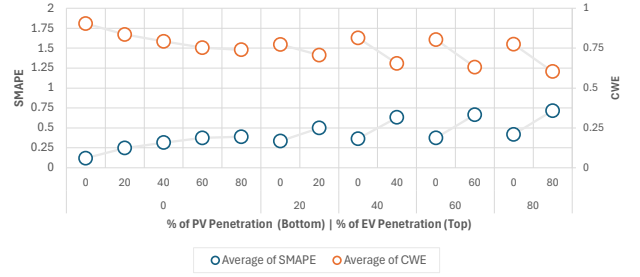


Figure 3: Variation of performance for active power.

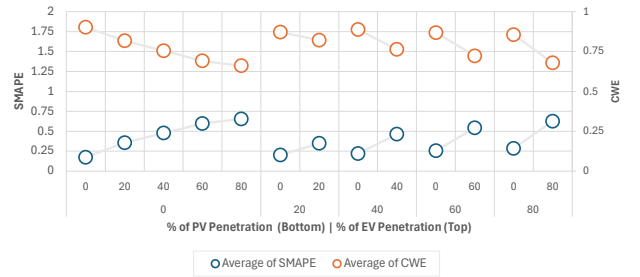


Figure 4: Variation of performance for reactive power.

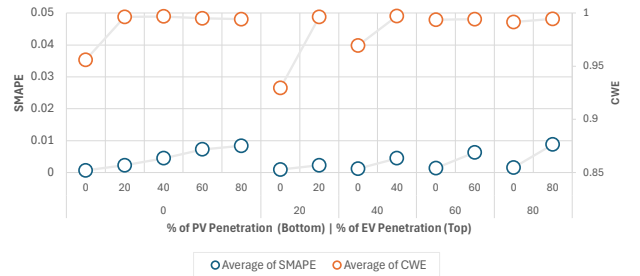


Figure 5: Variation of performance for voltage.

To further illustrate the voltage forecasting results, Fig. 6 presents the outcomes for the 80% PV - 80% EV scenario over a seven-day period. It becomes evident that there is a significant daily voltage drop, which the forecasting model occasionally fails to capture fully. Still, it is important to remark that the predictive interval often includes the true value, as expected per the results of CWE in Fig. 5.

## 5. CONCLUSION

The paper presents a framework for multivariate probabilistic forecasting of active power, reactive power, and voltage in LV secondary substations, evaluated across simulated scenarios with varying PV and EV penetration levels. Results indicate significant degradation in

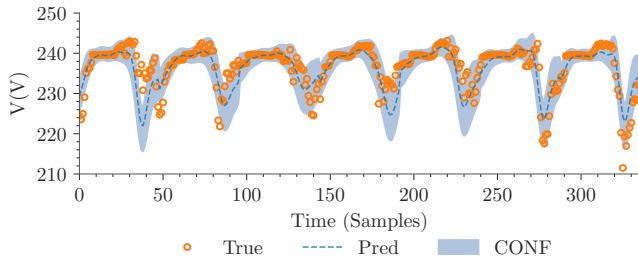


Figure 6: Seven days of voltage forecast in the 80% PV and EV penetration scenario.

active and reactive power forecasts with higher EV penetration, particularly at 80% levels, while voltage forecasting is less affected by PV but declines with increased EV penetration. Future work should include empirical validation to better understand real-world system responses and enhance forecasting accuracy and resilience assessment.

## ACKNOWLEDGMENTS

This work was supported by Eaton Corporation's Center for Intelligent Power (CIP), Dublin, Ireland (AF). This work is funded by FCT projects 10.54499/2022.15771.MIT; 10.54499/LA/P/0083/2020; 10.54499/UIDP/50009/2020; 10.54499/UIDB/50009/2020; and 10.54499/EXPL/CCI-COM/1234/2021 (LP).

CIREC Workshop on Resilience of Electric Distribution Systems  
Chicago, November 7-8, 2024  
Paper n° 1118

## References

- [1] E. Hassanzadeh, M. E. Hajiabadi, M. Samadi, and H. Lotfi, "Improving the resilience of the distribution system using the automation of network switches," *The Journal of Engineering*, vol. 2023, no. 2, e12238, 2023.
- [2] P. Denholm, M. O'Connell, G. Brinkman, and J. Jorgenson, "Overgeneration from Solar Energy in California. A Field Guide to the Duck Chart," National Renewable Energy Lab. (NREL), Golden, CO (United States), Tech. Rep. NREL/TP-6A20-65023, Nov. 2015. DOI: 10.2172/1226167.
- [3] M. Sanjari and H. Karami, "Optimal control strategy of battery-integrated energy system considering load demand uncertainty," *Energy*, vol. 210, p. 118525, Nov. 2020. DOI: 10.1016/j.energy.2020.118525.
- [4] M. Yadav, N. Pal, and D. K. Saini, "Low voltage ride through capability for resilient electrical distribution system integrated with renewable energy resources," *Energy Reports*, vol. 9, 833–858, Dec. 2023, ISSN: 2352-4847. DOI: 10.1016/j.egy.2022.12.023.
- [5] U. Langenmayr, W. Wang, and P. Jochem, "Unit commitment of photovoltaic-battery systems: An advanced approach considering uncertainties from load, electric vehicles, and photovoltaic," *Applied Energy*, vol. 280, p. 115972, 2020.
- [6] M. Z. Oskouei, A. A. Şeker, S. Tunçel, et al., "A critical review on the impacts of energy storage systems and demand-side management strategies in the economic operation of renewable-based distribution network," *Sustainability*, vol. 14, no. 4, p. 2110, 2022.
- [7] M. Yilmaz and P. T. Krein, "Review of the impact of vehicle-to-grid technologies on distribution systems and utility interfaces," *IEEE Transactions on Power Electronics*, vol. 28, no. 12, pp. 5673–5689, 2013. DOI: 10.1109/TPEL.2012.2227500.
- [8] V. Astapov, S. Mishra, I. Palu, and S. Trashchenkov, "The role of electrical vehicles for power quality and security during outages in the distribution grid," in *2020 IEEE 61th International Scientific Conference on Power and Electrical Engineering of Riga Technical University (RTUCon)*, 2020, pp. 1–5. DOI: 10.1109/RTUCon51174.2020.9316604.
- [9] P. Yu, C. Wan, Y. Song, and Y. Jiang, "Distributed control of multi-energy storage systems for voltage regulation in distribution networks: A back-and-forth communication framework," *IEEE Transactions on Smart Grid*, vol. 12, no. 3, pp. 1964–1977, 2021. DOI: 10.1109/TSG.2020.3026930.
- [10] A. I. Nousedlis, G. C. Christoforidis, and G. K. Papagiannis, "Active power management in low voltage networks with high photovoltaics penetration based on prosumers' self-consumption," *Applied Energy*, vol. 229, 614–624, Nov. 2018, ISSN: 0306-2619. DOI: 10.1016/j.apenergy.2018.08.032.
- [11] T. Zufferey, S. Renggli, and G. Hug, "Probabilistic state forecasting and optimal voltage control in distribution grids under uncertainty," *Electric Power Systems Research*, vol. 188, p. 106562, Nov. 2020, ISSN: 0378-7796. DOI: 10.1016/j.epsr.2020.106562.
- [12] A. Faustine, N. J. Nunes, and L. Pereira, "Efficiency through simplicity: Mlp-based approach for net-load forecasting with uncertainty estimates in low-voltage distribution networks," *IEEE Transactions on Power Systems*, pp. 1–11, 2024. DOI: 10.1109/TPWRS.2024.3400123.

- [13] A. Bracale, P. Caramia, P. De Falco, and T. Hong, "A multivariate approach to probabilistic industrial load forecasting," *Electric Power Systems Research*, vol. 187, p. 106 430, 2020. DOI: 10.1016/j.epsr.2020.106430.
- [14] W. Zhang, H. Quan, O. Gandhi, R. Rajagopal, C.-W. Tan, and D. Srinivasan, "Improving Probabilistic Load Forecasting Using Quantile Regression NN With Skip Connections," *IEEE Transactions on Smart Grid*, vol. 11, no. 6, pp. 5442–5450, Nov. 2020, ISSN: 1949-3061. DOI: 10.1109/TSG.2020.2995777.
- [15] M. Deakin, D. Greenwood, S. Walker, and P. C. Taylor, "Hybrid european mv–lv network models for smart distribution network modelling," in *2021 IEEE Madrid PowerTech*, 2021, pp. 1–6. DOI: 10.1109/PowerTech46648.2021.9494860.
- [16] R. Fachrizal, U. H. Ramadhani, J. Munkhammar, and J. Widén, "Combined PV–EV hosting capacity assessment for a residential LV distribution grid with smart EV charging and PV curtailment," *Sustainable Energy, Grids and Networks*, vol. 26, p. 100 445, Jun. 2021. DOI: 10.1016/j.segan.2021.100445.
- [17] A. Faustine and L. Pereira, "Fpseq2q: Fully parameterized sequence to quantile regression for net-load forecasting with uncertainty estimates," *IEEE Transactions on Smart Grid*, vol. 13, no. 3, pp. 2440–2451, 2022. DOI: 10.1109/TSG.2022.3148699.